articles

molecular pharmaceutics

Hepatocyte Targeting of Nucleic Acid Complexes and Liposomes by a T7 Phage p17 Peptide

So C. Wong,[†] Darren Wakefield,[†] Jason Klein,[†] Sean D. Monahan,[†] David B. Rozema,[†] David L. Lewis,[†] Lori Higgs,[†] James Ludtke,[‡] Alex V. Sokoloff,[‡] and Jon A. Wolff*[,‡]

Mirus Bio Corporation, 505 South Rosa Road, Madison, Wisconsin 53719, and Department of Pediatrics and Department of Medical Genetics, Waisman Center, University of Wisconsin, 1500 Highland Avenue, Madison, Wisconsin 53719

Received November 28, 2005

Abstract: A critical step for liver-directed gene therapy is the selective targeting of nucleic acids to hepatocytes. We have previously discovered that the proximal half of the T7 phage tail fiber protein (p17) targeted intact T7 phage and recombinant proteins to hepatocytes in vivo. In the present study, we have localized the targeting activities to a 33 amino acid sequence within the p17 coiled-coil rod domain. Given that the tail fiber domain from which the peptide was derived may form α and triple helical structures, biophysical studies (CD spectra and analytical ultracentrifugation) were conducted to determine the secondary and tertiary structures of the peptide. This peptide is able to target proteins, polymers, and siRNA and also particles such as DNA polyplexes and liposomes to hepatocytes. A variety of coupling strategies and chemistries were employed, thus demonstrating that this peptide is a versatile system for delivering cargo. The ability of this hepatocyte-targeting peptide to target DNA-containing particles suggests that it should be useful in the development of both nonviral and viral vectors. However, biological function of delivered cargo has not been demonstrated. This was primarily due to failure of delivered cargo to escape the endosomes. Further studies are in progress to provide functional activity of delivered nucleic acids by enabling their endosomal escape.

Keywords: Hepatocyte; T7 phage; p17; tail fiber protein; targeting; siRNA; nucleic acid; liposome; gene delivery

Introduction

Given its central role in metabolism, the secretion of circulating proteins, and infectious disorders, a large number of genetic and acquired disorders are amenable to liver-directed gene therapy.[1−3] The recent discovery of RNA interference (RNAi) has opened promising approaches for treating dominant genetic disorders and viral hepatitis.[4−8] However, despite this promise, a safe and effective delivery method for transferring nucleic acid molecules to hepatocytes remains to be perfected. Both viral and nonviral vectors are being developed for this purpose.

A critical step for liver-directed gene therapy is the targeting of nucleic acids to hepatocytes. While the liver could be accessed by direct injection into liver vessels such

* Author to whom correspondence should be addressed. Mailing address: Waisman Center, 1500 Highland Avenue, Room 362, Madison, WI 53705. Tel: (608) 263-5993. Fax: (608) 263-0530. E-mail: jwolff@wisc.edu.

[†] Mirus Bio Corporation.

[‡] University of Wisconsin.

(1) Wu, J.; Nantz, M. H.; Zern, M. A. *Front. Biosci.* **2002**, *7*, d717−25.

(2) Ghosh, S. S.; Takahashi, M.; Thummala, N. R.; Parashar, B.; Chowdhury, N. R.; Chowdhury, J. R. *J. Hepatol.* **2000**, *32*, 238−52.

(3) Nguyen, T. H.; Ferry, N. *Gene Ther.* **2004**, *11* (Suppl. 1), S76−84.

(4) Tuschl, T.; Zamore, P. D.; Lehmann, R.; Bartel, D. P.; Sharp, P. A. *Genes Dev.* **1999**, *13*, 3191−7.

10.1021/mp050108r CCC: $33.50
Published on Web 03/28/2006

as the portal vein, bile duct, and hepatic vein or artery, a less invasive and therefore preferred route would be via a peripheral vein injection. If a nucleic acid would be injected into a peripheral vein, it would have to travel a circuitous path to eventually reach the liver. This would entail venous return to the right side of the heart, passage through the lung, return to the left side of the heart, ejection out of the heart via the aorta, entry into the liver sinusoids via the hepatic artery, and extravasation out of the liver sinusoids to access the hepatocytes. The nucleic acid would also have to avoid the Kupffer cells in the liver whose activation can be toxic.[9] While this long traverse would appear to be a daunting process, both viral and nonviral vectors have been shown to be able to make this journey.[3,10] The delivery pathway is aided by the presence of open pores (fenestrae), approximately 100 nm in diameter, in the liver sinusoids that allows direct access to hepatocyte cells and thus avoids the need for transcytosis through the endothelium.

In vivo delivery is aided by the inclusion of cell-specific ligands for the target cell.[11] For hepatocyte targeting, natural or synthetic ligands for the asiologlycoprotein receptor (ASGPr) have been widely used in many liver-targeted drug and gene delivery studies. While functional hepatocyte targeting with a small molecule drug[12] has been demonstrated, the utility of ASGPr ligands for targeting larger sized particulate cargo such as gene delivery and liposomal drug carriers has been less certain.[13−16] Cholesterol has also been used to target siRNA to hepaocytes.[17,18]

While synthetic or natural ligands of the asialoglycoprotein receptor (ASGPr) have been the mainstay of hepatocyte-targeting efforts, an additional targeting system would expand the gene therapist's armamentarium for enabling efficient delivery of nucleic acids to hepatocytes in vivo. Different ligands could utilize different uptake mechanisms. New ligands may be less threshold-dependent, more effective at lower concentrations, and more dose-responsive: all critical properties for reliable pharmaceutics. Gene transfer may be more effective depending on the receptor and its cognate uptake pathway. Different hepatocyte targeting ligands would enable delivery to diverse subcellular spaces that may be advantageous for nucleic acid delivery. Also, certain uptake pathways may be less affected by liver disorders such as inborn errors of metabolism, hepatitis, or cirrhosis.

In order to develop additional hepatocyte-targeting ligands, we have previously used a peptide library displayed on T7 phage, a ~60 nm icosahedral particle similar in size to gene delivery complexes.[19,20] Surprisingly, we discovered that the native T7 phage tail fiber protein (p17) mediated the rapid and selective uptake of intact T7 phage by rodents and primate hepatocytes in vivo.[20] The T7 phage tail complex consists of a conical tail tube that is surrounded by six kinked tail fibers. Each of the six kinked tail fibers of T7 phage contains a trimer of p17, a polypeptide of 553 residues.[21] Our studies indicated that the targeting signal was within residues 151−267 of the proximal half of the tail fiber that forms a coiled-coil, rodlike structure.[21] Recombinant protein expression studies demonstrated that this rod domain alone was able to mediate the accumulation of various p17 fusion proteins in hepatocytes in vivo.[20]

In the present study, we have further characterized the targeting determinant of the T7 tail fiber protein and have localized the targeting activities to a peptide of 33 amino acids within the p17 rod domain. We demonstrated that this peptide can target small molecules, proteins, and siRNA and also particles such as DNA polyplexes and liposomes to hepatocytes. To the best of our knowledge, a functional hepatocyte-targeting peptide has heretofore not been described.

Materials and Methods

Peptide Synthesis. Peptides were synthesized using standard solid phase FMOC chemistry and an Applied

(5) Morrissey, D. V.; Lockridge, J. A.; Shaw, L.; Blanchard, K.; Jensen, K.; Breen, W.; Hartsough, K.; Machemer, L.; Radka, S.; Jadhav, V.; Vaish, N.; Zinnen, S.; Vargeese, C.; Bowman, K.; Shaffer, C. S.; Jeffs, L. B.; Judge, A.; Maclachlan, I.; Polisky, B. *Nat. Biotechnol.* **2005**, *23* (8), 1002−7.

(6) McCaffrey, A. P.; Meuse, L.; Pham, T. T.; Conklin, D. S.; Hannon, G. J.; Kay, M. A. *Nature* **2002**, *418*, 38−9.

(7) Fire, A.; Xu, S.; Montgomery, M. K.; Kostas, S. A.; Driver, S. E.; Mello, C. C. *Nature* **1998**, *391*, 806−11.

(8) Crombie, C.; Fraser, A. *Lancet* **2005**, *365*, 1288−90.

(9) Lieber, A.; He, C. Y.; Meuse, L.; Schowalter, D.; Kirillova, I.; Winther, B.; Kay, M. A. *J. Virol.* **1997**, *71*, 8798−807.

(10) Pfeifer, A.; Verma, I. M. *Annu. Rev. Genomics Hum. Genet.* **2001**, *2*, 177−211.

(11) Meijer, D. K.; Molema, G. *Semin. Liver Dis.* **1995**, *15*, 202−56.

(12) Seymour, L. W.; Ferry, D. R.; Anderson, D.; Hesslewood, S.; Julyan, P. J.; Poyner, R.; Doran, J.; Young, A. M.; Burtles, S.; Kerr, D. J. *J. Clin. Oncol.* **2002**, *20*, 1668−76.

(13) Rensen, P. C.; Sliedregt, L. A.; Ferns, M.; Kieviet, E.; van Rossenberg, S. M.; van Leeuwen, S. H.; van Berkel, T. J.; Biessen, E. A. *J. Biol. Chem.* **2001**, *276*, 37577−84.

(14) Biessen, E. A. L.; Bakkeren, H. F.; Beuting, D. M.; Kuiper, J.; van Berkel, T. J. C. *Biochem. J.* **1994**, *299*, 291−6.

(15) Lee, Y. C.; Townsend, R. R.; Hardy, M. R.; Longren, J.; Arnarp, J.; Haraldsson, M.; Lonn, H. *J. Biol. Chem.* **1983**, *258*, 199−202.

(16) Fiume, L.; Cerenzia, M. R.; Bonino, F.; Busi, C.; Mattioli, A.; Brunetto, M. R.; Chiaberge, E.; Verme, G. *Lancet* **1988**, *2*, 13−5.

(17) Lorenz, C.; Hadwiger, P.; John, M.; Vornlocher, H. P.; Unverzagt, C. *Bioorg. Med. Chem. Lett.* **2004**, *14*, 4975−7.

(18) Soutschek, J.; Akinc, A.; Bramlage, B.; Charisse, K.; Constien, R.; Donoghue, M.; Elbashir, S.; Geick, A.; Hadwiger, P.; Harborth, J.; John, M.; Kesavan, V.; Lavine, G.; Pandey, R. K.; Racie, T.; Rajeev, K. G.; Rohl, I.; Toudjarska, I.; Wang, G.; Wuschko, S.; Bumcrot, D.; Koteliansky, V.; Limmer, S.; Manoharan, M.; Vornlocher, H. P. *Nature* **2004**, *432*, 173−8.

(19) Sokoloff, A. V.; Bock, I.; Zhang, G.; Hoffman, S.; Dama, J.; Ludtke, J. J.; Cooke, A. M.; Wolff, J. A. *Mol. Ther.* **2001**, *3*, 821−30.

(20) Sokoloff, A. V.; Wong, S. C.; Ludtke, J. J.; Sebestyen, M. G.; Subbotin, V. M.; Zhang, G.; Budker, T.; Bachhuber, M.; Sumita, Y.; Wolff, J. A. *Mol. Ther.* **2003**, *8*, 867−72.

(21) Studier, F. W. *Virology* **1969**, *39*, 562−74.

Biosystems 433A automated peptide synthesizer. All amino acids and derivatives were purchased from Novabiochem (La Jolla, CA). For biotinylated or N-terminus cysteine peptide synthesis, FMOC-aminoethyl-*O*′(2-carboxyethyl) undecaethylene glycol (FMOC-NH-PEG11-OH) was incorporated at the amino terminus of the peptide. The FMOC-NH-PEG11-peptide was deprotected with piperidine, and the resulting amine was either biotinylated using 5-(2-oxohexahydrothieno[3,4-*d*]imidazol-6-yl)pentanoic acid 2,5-dioxopyrrolidin-1-yl ester (biotin *N*-hydroxysuccimide ester) to afford the biotin-PEG11-peptide or modified with FMOC-Cys(trt)-OH to generate the cysteine-PEG11-peptide. The modified peptides were then further subjected to standard cleavage and deprotection using trifluoroacetic acid (TFA). The peptides were HPLC purified and analyzed by mass spectrometry.

Experimental Animals. ICR mice (20−30 g) were purchased from Harlan Spraque Dawley (Indianapolis, IN). All experiments were performed in accordance with a protocol approved by the Institutional Animal Care and Use Committee.

Biotinylated Peptide Functional Testing. For screening of hepatocyte targeting functions of biotinylated peptides MC893 and MC910, peptides were mixed with 100 μg of Cy3-SA (Jackson ImmunoResearch Laboratories, Inc., West Grove, PA) (SA, streptavidin) at molar ratios of 4:1, 9:1, 12:1, 18:1, or 30:1 in a solution containing 10 mM HEPES, 150 mM NaCl, pH 8. All other biotinylated peptides were tested at molar ratios of 12:1 only. The mixtures (in 250 μL) were injected into mice via the tail vein. Animals were sacrificed 10 or 20 min after injection, and liver samples were excised. For some experiments, tissue samples from lung, kidney, spleen, and heart were also excised. Tissue samples were frozen in OCT freezing media (Fisher Scientific), and frozen tissue sections (5−7 μm) were prepared using a Microm HM 505N cryostat (Carl Zeiss) and placed onto Superfrost-Plus microscope slides (Fisher Scientific). Tissue sections were fixed in PBS containing 4% formalin for 20 min and counterstained with Alexa-488 phalloidin (13 nM, Molecular Probes, Eugene, OR) and To-Pro-3 (20 nM, Molecular Probes) in PBS for 20 min. Processed slides were mounted in Vectorshield (Vector Laboratories, Burlingame, CA) and analyzed by a LSM510 confocal microscope (Carl Zeiss, Thornwood, NY).

Analytical Ultracentrifugation. Sedimentation equilibrium experiments were conducted at 20 °C in a Beckman-Optima XL-An analytical ultracentrifuge (Beckman Instruments, Palo Alto, CA). One hundred microliter peptide solutions at 4.5−272 μM in PBS were equilibrated for 48 h at 8 speeds in the range from 3000 to 60 000 rpm. Plots of ln(A) vs R^2, where A is absorbance at 280 nm and R^2 is radial position in cm^2, produced a series of straight lines with slopes proportional to the MW.

Circular Dichroism Spectroscopy. CD measurements were made using an AVIV 62A DS circular dichroism spectrometer (AVIV associates, NJ). Peptide solutions at 120 μM were prepared in PBS and were examined in 5 mm quartz cuvettes. Spectra were recorded at 22 °C using 1 nm intervals. After baseline correction, ellipticities in mdeg were converted to molar ellipticities (deg cm^2 dmol^{-1}) by normalizing for the concentration of peptide bonds.

Preparation of T7 Peptide Streptavidin Conjugates for Biotinylated Cargo Delivery. Two milligrams of SA (Jackson ImmunoResearch Laboratories) was dissolved in 200 μL of dH_2O and added to a 200 μL solution of 100 mM sodium phosphate, 300 mM NaCl, 2 mM EDTA, pH 7.2. *N*-Succinimidyl 3-[2-pyridyldithio]propionate (20 molar equiv) (SPDP, Pierce Biotechnology Inc., Rockford, IL) dissolved in DMF at 10 mg/mL was then added to the SA solution and mixed at room temperature for 1 h. The SPDP-modified streptavidin was then purified using a G-25 Sephadex column. The number of PDP groups per SA molecule was determined by measuring the release of pyridine-2-thione (OD_{280} = 5100 M^{-1} cm^{-1}) under reducing conditions. The SA-PDP was added to MC920 or MC993 at a 1:3 molar ratio and incubated for 24 h or longer at 4 °C. The MC920-SA and MC993-SA conjugates were then purified on a G-25 Sephadex column. The sample was then freeze-dried and dissolved in a solution of 25 mM MES, 125 mM NaCl, pH 6.5 at 3 mg/mL.

Preparation and Injection of Biotinylated Cy3-Dextran (70 kDa) and Biotinylated Cy3-siRNA. Cy3-labeled biotinylated dextran was synthesized in a two-step process. First, aminodextran (Molecular Probes, 70 kDa, 17.9 mol of NH_2 per polymer) was biotinylated using the NHS-PEO_4-biotin reagent (Pierce Biotechnology Inc.). The biotinylated dextran was then dialyzed to remove excess reagents, lyophilized, and then dissolved in dH_2O at 30 mg/mL and fluorescently labeled with Cy3-OSu (Amersham) at a molar ratio of 1:8. Excess unincorporated Cy3 dye was removed from biotinylated Cy3-labeled dextran using a Sephadex G-50 column. The sample was freeze-dried and dissolved at 7.5 mg/mL in a solution containing 25 mM HEPES, 125 mM NaCl, pH 8.0.

For in vivo injections, 25 μg of MC892-SA conjugate was mixed with biotinylated Cy3-dextran at a SA/biotin molar ratio of 1:1 in 400 μL of 10 mM HEPES buffer, pH 8, containing 150 mM of NaCl. Samples were injected into mice via the tail vein. The same amount of biotinylated Cy3-labeled dextran without MC892-SA added was injected to determine the level of nonspecific delivery. For siRNA targeting experiments, MC892-SA (23 μg) was mixed with 30 μg of Cy3-labeled (Cy3 Label*IT*, Mirus Bio Corporation) biotinylated siRNA, a double-stranded, 21-nucleotide-long, anti-luciferase sequence with two overhanging 5′ nucleotides at each end, in 250 μL of 10 mM HEPES buffer, pH 8, containing 150 mM of NaCl. Sense strand: biotin-CUUACGCUGAGUACUUCGAdTdT. Antisense strand: UCGAAGUACUCAGCGUAAGdTdT (Dharmacon, Lafayette, CO). Liver samples were removed at 10 or 20 min after injection. Samples from Cy3-dextran injected mice were frozen in OCT freezing media. Samples from siRNA injected mice were fixed in 4% paraformaldehyde in PBS overnight and then put into a 30% sucrose/PBS solution until samples

settled to the bottom. Liver samples were then frozen in OCT freezing medium. Frozen liver sections were prepared and analyzed by confocal microscopy as described above.

For in vivo gene knockdown experiments, biotinylated anti-PPARa siRNA (Dharmacon) was used instead of anti-luciferase siRNA. Sense strand: biotin-GAUCGGAGCUG-CAAGAUUCdTdT. Anti-sense strand: P-GAAUCUUG-CAGCUCCGAUCdTdT (5′ end was phosphorylated). MC892-SA conjugate and biotinylated anti-PPARa siRNA mixtures were injected as described above for Cy3-labeled siRNA targeting experiments. Liver was removed 24 h after injection for total RNA isolation using the TRIzol Reagent (Molecular Research Center, Inc., Cincinnati, OH).

Quantitative Real-Time PCR and Luciferase Assays. (A) Quantitative Real-Time PCR. Total RNA from liver was quantitated using a SPECTRAmax Plus spectrophotometer (Molecular Devices). Total RNA (500 ng) was reverse transcribed using SuperScript III (Invitrogen) and oligo-dT primers according to the manufacturer's protocol.

Quantitation of gene-specific mRNA levels was performed by qRT-PCR using an iCycler iQ system (BioRad). Relative levels of *PPAR*α and *GAPDH* were measured in biplex reactions performed in triplicate using TaqMan Universal PCR Master Mix and the TaqMan Gene Expression Assay for *PPAR*α (Catalog No. Mm00440939_m1, Applied Biosystems, Foster City, CA) following the manufacturer's protocol. The *GAPDH* primers and probe (Integrated DNA technologies, Coralville, IA) were *GAPDH*-forward 5′-AAATGGTGAAGGTCGGTGTG-3′; *GAPDH*-reverse 5′-CATGTAGTTGAGGTCAATGAAGG-3′; probe 5′-Hex/CGTGCCGCCTGGAGAAACCTGCC/BHQ-3′.

(B) Luciferase Assays. Gene knockdown activities of biotinylated modified siRNA were tested in cultured cell transfection assays. Biotinylated anti-luciferase siRNA was transfected into Hepa-luc cells using the *Trans*IT TKO transfection reagent (Mirus Bio Corporation, Madison, WI) according to recommended protocol. The Hepa-luc mouse hepatocyte cell line was a derivative of Hepa1clc-7 hepatoma cells (ATCC, Manassas, VA) with the gene encoding firefly luciferase integrated in its genome. Cells were harvested 24 h after transfection, cell lysates were prepared, and luciferase activity was measured using a kit from Promega (Madison, WI) following the manufacturer's recommendation.

Direct Conjugation of T7 Peptide to Dextran. Amino-dextran (70 kDa, Invitrogen) was modified with 50 molar equiv, relative to dextran, of SPDP (Pierce) cross-linking reagent in 5 mM HEPES buffer pH 7.5. After 1 h of reaction, the dextran was dialyzed to remove any uncoupled SPDP. The amount of coupled PDP groups was quantified as described above and was determined to be 18 per dextran. The PDP-dextran (500 μg) was then labeled with 25 nmol of thiol reactive Cy3 dye and 300 μg of cysteine-containing peptide MC892.

Cy3-dextran-MC892 conjugate (500 μg of dextran) was injected into mice via the tail vein in 250 μL, liver samples were removed 10 min after injection for frozen section preparation, and tissue sections were counterstained and analyzed using confocal microscopy as described above. Cy3-PDP-dextran injected without MC892 was used as control.

Preparation of Plasmid DNA Complexes and Injection. (A) Complex Formulation. The membrane lytic pBAVE polymer was synthesized as previously described.[22] To prepare pBAVE polymer for T7-SA conjugate targeted DNA particle delivery, 15% of the amino groups in pBAVE were modified with *N*-hydroxysuccimide ester (NHS)-PEG_{5000}-methoxy (12.5%) and NHS-PEG_{5000}-biotin (2.5%). All NHS-PEG molecules were purchased from Nektar Therapeutics (San Carlos, CA). Luciferase expressing plasmid DNA pMIR48, which expresses the firefly gene (Luc+, Promega, Madison, WI), was labeled with Cy3-Label*IT* (Mirus Bio Corporation) according to the recommended procedures. The modified pBAVE derivative (pBAVE-PEG-biotin/methoxy) was added to Cy3-DNA at a weight ratio of 4:1 (pBAVE/DNA) in 400 μL of 5 mM HEPES, 290 mM glucose, pH 8. Complexes were cross-linked for 3 h at room temperature with 1 molar equiv of glutaraldehyde (relative to pBAVE amines).

(B) Modification of DNA Complexes with CDM-PEG_{500}. Ten minutes prior to the injection of DNA complexes, 2 wt equiv of CDM-PEG_{500} (relative to pBAVE in complexes) was added to modify the ζ-potentials of the cross-linked DNA complexes. The synthesis of 2-propionic-3-methylmaleic anhydride (CDM) has been previously described.[23] To synthesize CDM-PEG_{500}, CDM was converted to CDM acid chloride according to published procedures.[24] Briefly, a 3−5 molar excess of oxalyl chloride was added to a dichloromethane solution of CDM. This solution was stirred overnight and solvent removed by rotary evaporation. The resulting oil was placed under high vacuum for 1 h. The resulting acid chloride was dissolved in dichloromethane. To this solution was added 1.1 molar equiv of methoxy-PEG_{500}-NH_2, prepared from MeO-PEG-OH (Fluka) according to published procedures,[25] and 2 molar equiv of pyridine. The solution was stirred for several hours and the solvent removed by rotary evaporation. This crude reaction mixture was then dissolved in 4−5 mL of water and purified by reverse phase HPLC. The purified CDM-PEG_{500} was lyophilized and dissolved in ethanol at 100 mg/mL.

(C) Injection of Complexes into Mice. For in vivo hepatocyte targeting experiments, SA-MC892 conjugate was added to the CDM-PEG_{500} modified DNA or siRNA complexes at a SA to biotin molar ratio of 1:1 immediately before injection. For each injection, 20 μg of DNA or siRNA containing complexes in 250 μL of the formulation buffer was injected into mice via the tail vein. One hour after

(22) Wakefield, D. H.; Klein, J. J.; Wolff, J. A.; Rozema, D. B. *Bioconjugate Chem.* **2005**, *16*, 1204−8.
(23) Rozema, D. B.; Ekena, K.; Lewis, D. L.; Loomis, A. G.; Wolff, J. A. *Bioconjugate Chem.* **2003**, *14*, 51−7.
(24) Naganawa, A.; Ichikawa, Y.; Isobe, M. T. *Tetrahedron* **1994**, *21*, 8969.
(25) Aronov, O.; Horowitz, A. T.; Gabizon, A.; Gibson, D. *Bioconjugate Chem.* **2003**, *14*, 563−74.

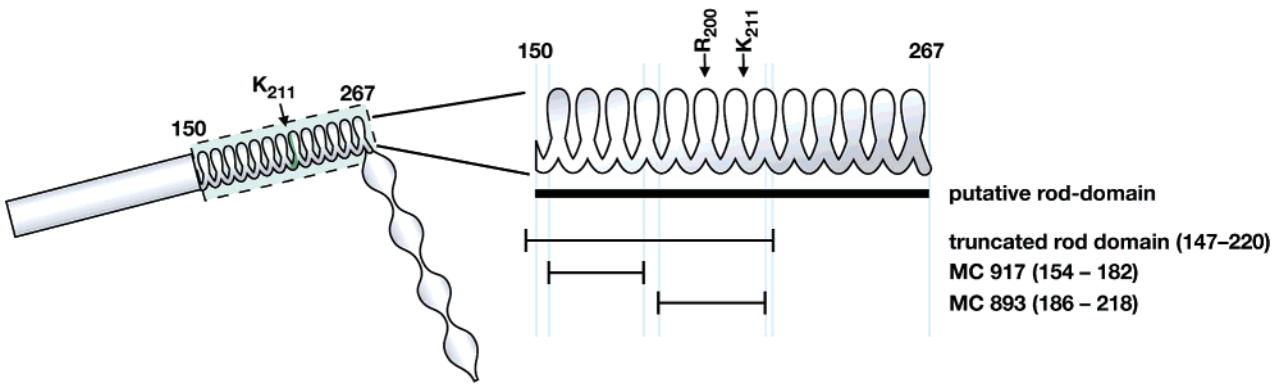

Figure 1. A schematic diagram of the T7 tail fiber. The relative locations of putative rod domain, the recombinant truncated rod-domain fragment (residues 147−220), and the p17 synthetic peptides MC893 and MC917 are indicated.

injection, liver samples were removed. Frozen liver sections were prepared and analyzed by confocal microscopy as described above.

Measurement of Particle Sizes and ζ-Potential. The size and ζ-potential of cross-linked complexes with and without CDM-PEG_{500} modification were determined using a ZetaPals particle analyzer (Brookhaven Instrument Corp., Huntsville, NY).

Liposome Formulation and Injection. Unilamellar liposomes were prepared by the extrusion method. Briefly, 7 mg of lipid mixture (mole % composition: 1% DSPE-PEG2000-biotin, 4% DSPE-PEG2000-methoxy, 30% cholesterol, 65% DOPC, and 0.5% Oregon Green-DHPE) was dissolved in chloroform, mixed in a 50 mL round-bottom flask, and dried under vacuum. The small amount of Oregon Green-DHPE (Molecular Probes, Eugene, OR) was included for lipid concentration determination. Cy3-hydrazine (Amersham Biosciences, Piscataway, NJ), 25 mg in 1 mL of methanol, was then added to the dried lipid, dried under vacuum, and then lyophilized for at least 2 h. The lipid film was rehydrated by addition of 0.7 mL of buffer (10 mM HEPES pH 7.5, 150 mM NaCl) and mixed for 15−20 min. The liposome preparation was then bath sonicated for 30 min. Using a Lipex extruder (Northern Lipid Inc., Vancouver, BC, Canada), liposomes were passed through a 100 nm polycarbonate membrane 5 times and followed by extruding through two layers of 50 nm hydrocarbonate membranes 10−15 times under pressure (700 psi).

Unincorporated Cy3-hydrazine was separated from the loaded liposomes on a Sepharose G-50 column. Unloaded liposomes were prepared for size and ζ-potential measurements using a Zeta-Plus particle analyzer (Brookhaven Instrument Corp., Huntsville, NY). The cyanine dye-hydrazide loaded liposomes were not sized due to interference of their fluorescence with the measurement. The concentration of lipid was calculated by measuring the Oregon Green fluorescence in liposomes recovered after the extrusion and purification procedures. To determine the loading efficiency, encapsulated cyanine dye-hydrazide was extracted from purified liposomes in methanol. The loading efficiency was calculated by the following equation: (recovered fluorescence/fluorescence in the starting lipid mixture) × 100. Five minutes before injection into mice, 100 μg of MC920-SA was added to half of the prepared liposomes. For control, 100 μg of nontargeting conjugate, MC910-SA, was added to the remaining liposomes prior to injection. The liposome and conjugate mixtures, in 250 μL, were injected into mice via the tail vein. Thirty minutes after injection, livers were gently perfused with PBS and 0.5 cm tissue blocks were excised and fixed overnight in PBS solution containing 4% paraformaldehyde. The following day, liver samples were equilibrated in a 30% sucrose solution and then embedded in OCT freezing medium and snap frozen in liquid nitrogen. Frozen liver sections were prepared and analyzed by confocal microscopy as described above.

Results and Discussion

Selection of p17-Derived Peptide Sequences. Two peptide sequences were selected for synthesis, a peptide of 29 amino acids derived from sequence 154−182 and a peptide of 33 amino acids derived from sequence186−218. The latter peptide was chosen on the basis of previous phage mutation and recombinant protein studies[20] (Figure 1). These mutation studies showed that a single point mutation at residue 211 in the p17 rod domain (a K/E_{211} substitution) abolished the hepatocyte-targeting activity.[20] In addition to the K/E_{211} mutation, it was also shown that T7 phage clones containing single point mutations in the p17 protein at R/L_{207}, R/C_{200} or R/S_{200} also resulted in inactivation of p17 liver-targeting function. Initial recombinant protein studies indicated that the p17 sequence 150−289, which contain the entire putative rod domain (sequence 151−267) of the p17 tail fiber protein, was sufficient to target various fusion proteins to hepatocytes.[20] Subsequently, a recombinant truncated rod-domain fragment (sequence 147−220) was shown to retain hepatocyte-targeting activity (data not shown). These observations strengthened our earlier reasoning that the targeting signal may be located within 2−3 heptad repeats of the p17 rod domain. Hence, to further elucidate the minimal functional targeting determinant, shorter p17 peptides based on the rod-domain sequence were chemically synthesized. These two peptides essentially represented the entire truncated rod-domain fragment (sequence 147−220) which was shown to contain the targeting determinant.

Table 1. Synthetic T7 Peptide Sequence ID and Functional Screening

peptide ID	N-terminus functional group	peptide sequence		targeting activities[a]
		sequence	location	
MC917	biotin-PEG11	LKTMNQNSWQARNEALQFRNEAETFRNQA	154−182	none
MC893	biotin-PEG11	KNESSTNATNTKQWRDETKGFRDEAKRFKNTAG	186−218	very good
MC949	biotin-PEG11	NESSTNATNTKQWRDETKGFRDEAKRFKNTAG	187−218	none
MC948	biotin-PEG11	ESSTNATNTKQWRDETKGFRDEAKRFKNTAG	188−218	weak
MC947	biotin-PEG11	SSTNATNTKQWRDETKGFRDEAKRFKNTAG	189−218	weak
MC992	biotin-PEG11	KNESSTNATNTKQWRDETKGFRDEAKRF	186−210	none
MC915	biotin-PEG11	KQWRDETKGFRDEAKRFKNTAG	197−218	none
MC910	biotin-PEG11	KNESSTNATNTKQWRDETKGFRDEAERFKNTAG	186−218 (K/E_{211})	weak
MC919	biotin-PEG11	KNESSTNATNTKQWRDETKGFRDEARRFKNTAG	186−218 (K/R_{211})	very good
MC929	biotin-PEG11	KNESSTNATNTKQWKDETKGFRDEAKRFKNTAG	186−218 (R/K_{200})	good
MC936	biotin-PEG11	RNESSTNATNTKQWRDETKGFRDEARRFRNTAG	186−218 ($K/R_{186,211,214}$)	none
MC937	biotin-PEG11	KNESSTNATNTRQWRDETRGFRDEARRFKNTAG	186−218 ($K/R_{197,204,211}$)	none
MC892	Cys-PEG11	KNESSTNATNTKQWRDETKGFRDEAKRFKNTAG	186−218	very good

[a] Targeting activities of p17 peptides were estimated by the average number of punctate Cy3-labeled SA or dextran (MC892) signals in hepatocytes in representative areas; very good = >50, good = 25−50, weak = 10−25, very weak = <10. Peptides were evaluated at 12:1 (peptide:SA) molar ratios.

The flexibility in chemical synthesis and design of p17 peptides also facilitated the incorporation of functional groups for coupling the targeting peptide to cargoes to be delivered. A biotin functional group was attached to the N-terminus of the p17 peptides. A small poly(ethylene glycol) (PEG) spacer was inserted between the biotin group and the peptide to enhance flexibility and accessibility for receptor binding. This synthetic approach allows the use of fluorescently labeled streptavidin (Cy3-SA) as a reporter molecule to monitor targeting activities. The biotinylated peptide derived from sequence154−182 was designated MC917, and from sequence 186−218, it was designated MC893 (Table 1).

Biotinylated Synthetic p17 Peptides Deliver Cy3-SA to Mouse Hepatocytes. The targeting activity of biotinylated p17 peptide was tested by mixing it with Cy3-SA at various molar ratios and injecting the complexes into mice via the tail vein. This indirect conjugation approach is depicted schematically in Figure 2, panel A. The hepatocyte-targeting efficiency of p17 peptide was evaluated by confocal microscopy. Relative targeting efficiencies were assessed, using a scoring system, by the average number of punctate signals found in hepatocytes in three representative images; each has a sampling surface area of 75 μm in a 4 μm thick section (Table 1). At 10 min after injection, at T7 peptide MC893 and Cy3-SA molar ratio of 12:1, a large number of punctate Cy3-SA signals were detected in most hepatocytes (Figure 3A). Nevertheless, a significant level of Cy3-SA was also found in areas outside of the hepatocytes. Whether these signals were on the hepatocyte cell membrane, in the space of Disse, or in sinusoidal cells could not be unambiguously determined. Optimal hepatocyte targeting occurred at a peptide:Cy3-SA molar ratio of 12:1. Cy3-SA bound to biotin alone was found only in sinusoidal cells (Figure 3B).

In agreement with our original observation in phage library screening,[20] the p17 peptide MC910, sequence 186−218 containing a K/E_{211} substitution, showed very little Cy3-SA signal in hepatocytes (Figure 3C) (Table 1). In addition, p17 peptide MC917 (sequence 154−182, Table 1), which was derived from the N-terminus of the rod domain, had no hepatocyte-targeting activity (Figures 1 and 3D). Peptide MC930 (sequence 186−225), a peptide with additional residues at the C-terminus, yielded no improvements on targeting efficiencies (data not shown). These results suggest that sequence 186−218 likely contained the entire targeting domain. These results also established the functional utility of the biotin/SA system as conjugation partners.

Besides the liver, Cy3-SA distribution was also examined in other organs. At 10 min after injection, Cy3-SA signal was found in spleen but at a much lower level than in liver and was mostly associated with the red pulp areas which consist of splenic capillary sinusoids interwoven with connective tissues (not shown). In the kidney, lung, and heart, Cy3-SA signal was barely above background (not shown). Most of the nonliver Cy3-SA signal was associated within blood vessels, suggesting that some of the signals were still in circulation 10 min after injection.

While the hepatocyte Cy3-SA signal was punctate at 10 min after injection, by 20 min after injection, the hepatocyte signal became more diffuse and there appeared a hazy cytoplasmic distribution of Cy3 fluorescence (not shown). This was likely a result of lysosomal degradation of endocytosed Cy3-SA and leakage of degraded fluorescent fragments into the cytoplasm. At 20 min after injection, nearly all the sinusoidal signal in liver was cleared.

Further Characterization of the Targeting Determinant. (A) Attempts To Shorten the Targeting Peptide. To further characterize the targeting determinant, we evaluated if the targeting peptide, sequence 186−218, could be shortened. Minimizing the targeting determinant would not only reduce the time and cost of peptide synthesis but also provide further information regarding the structure−function relationship of the peptide. To our surprise, removal of a single residue from the MC893 sequence at the N-terminus (MC949, residues 187−218) completely abolished the hepatocyte Cy3-SA targeting activities. Interestingly, peptides with additional residues deleted from the N-terminus (MC948

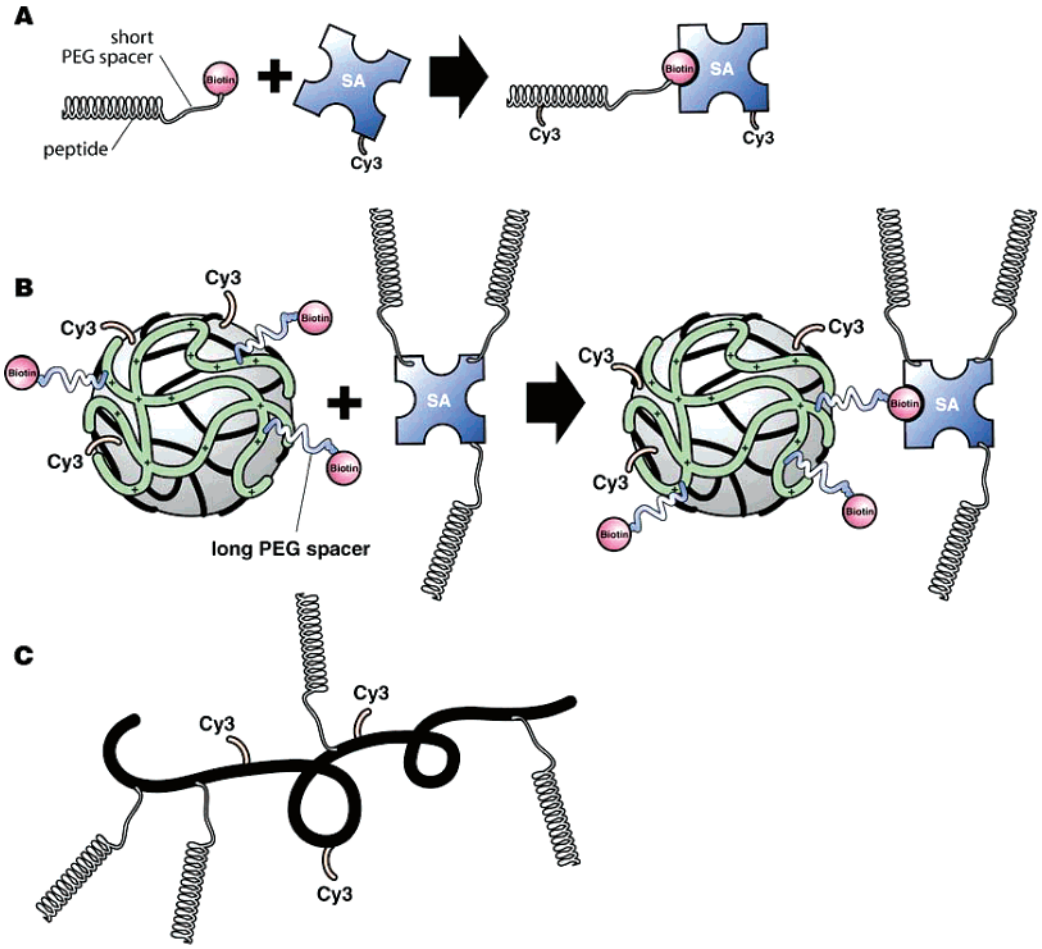

Figure 2. An illustration of the various p17 peptide conjugation approaches. (A) Complexation of biotinylated peptide to Cy3-labeled streptavidin (SA). (B) Complexation of biotinylated DNA polyplex to p17 peptide-SA conjugate. (C) Direct conjugation of p17 peptide to Cy3-labeled dextran.

or MC947) were weakly active (Table 1). This observation suggested that K_{186} may play a critical role in receptor interaction, while further deletions may have exposed or stabilized secondary binding characteristics. Nevertheless, liver-targeting activities of p17 peptides with further deletions at the N-terminus (MC915, residues 197−218) or C-terminus (MC992, residues 186−213) were completely abolished (Table 1). These results suggest that these regions contain critical residues that are required for specific ligand−receptor binding. On the other hand, a critical peptide length may have been required to maintain more general structural constraints for receptor interaction.

(B) Substituting Lysine Residues with Arginine Residues. Within the targeting peptide sequence (sequence 186−218) there were contained five lysine residues that occupied the exterior *b* and *e* positions in the tail fiber triple α-helical coiled-coil heptad repeats.[20] We were interested to determine if a conservative substitution of these lysine residues with arginine would affect hepatocyte targeting because a lysine-free peptide would enable amino reactive conjugation chemistry to be employed for cargo attachment without inactivating targeting activities. A series of p17 peptides with substitution of lysine by arginine were synthesized, and the targeting activities of these peptides were evaluated using Cy3-SA as a reporter molecule. Biotinylated p17 peptide with a single point substitution at K/R_{211} (MC919; Table 1) did not affect targeting activity when compared to the consensus sequence MC893; in fact, K/R_{211} substitution seems to have slightly improved hepatocyte-targeting efficiency. In agreement with this observation, the targeting activities were not significantly affected in five T7 phage clones where only one of the five p17 lysines was changed to arginine by site-directed mutagenesis (data not shown). However, biotinylated p17 peptide with multiple lysines to arginine substitutions such as K_{197}, K_{204}, and K_{211} to R (MC 937) or K_{186}, K_{211}, or K_{214} to R (MC936) failed to target Cy3-SA to hepatocytes. It is unclear why a single arginine substitution at all the lysine sites was tolerated but not multiple substitutions. Possibly, substitution at multiple sites significantly changed the structure of the peptide and adversely altered the efficiency of ligand receptor interaction or recognition.

Biophysical Characteristics of p17 Peptide by Circular Dichroism Spectroscopy and Analytical Ultracentrifugation. Purified recombinant p17 protein spontaneously assembles into trimers, the native conformation found in T7 phage tail fibers.[21] Since the targeting sequence was located within the α-helical coiled-coiled rod domain of p17, circular dichroism (CD) and analytical ultracentrifugation studies

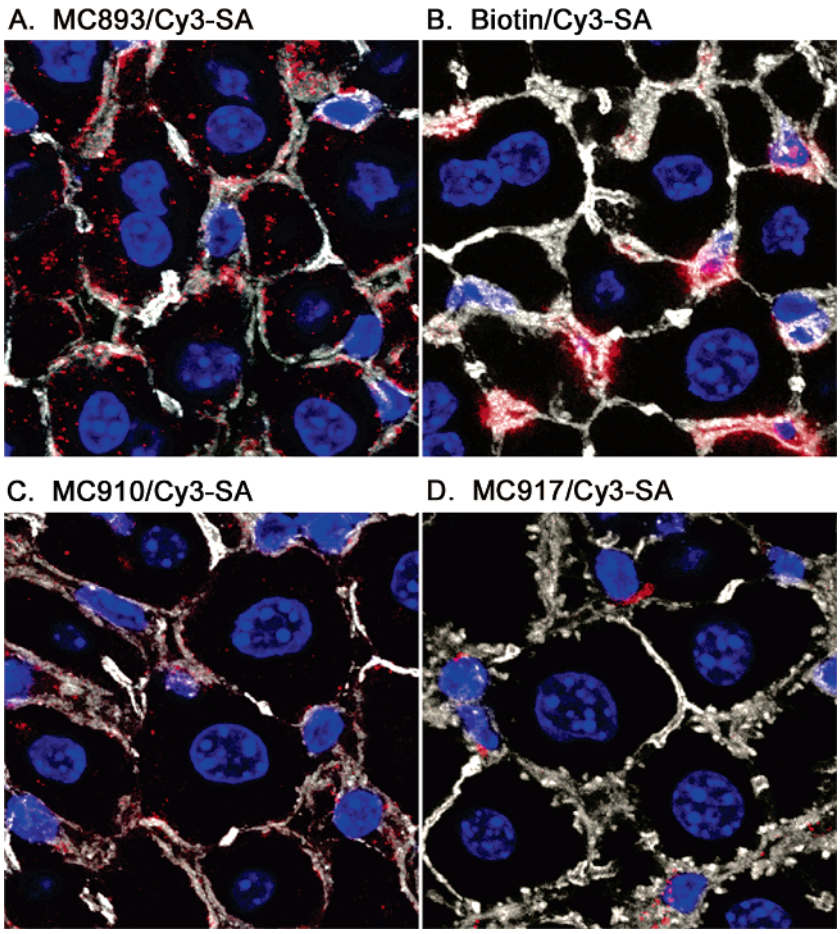

Figure 3. Synthetic biotinylated p17 peptide delivers Cy3-labeled SA (red) to hepatocytes. Liver samples were collected 10 min after tail vein injection. Images represent a flattened projection of 10 confocal optical sections, each 0.4 um thick. F-actin appears gray or white, and cell nuclei are blue.

were used to determine if MC893 peptides retain the α-helical structure and also assemble into trimers. CD spectral analysis results indicated that peptide MC893 did not exhibit any characteristic α-helical structure (data not shown). Furthermore, MC893 peptide existed in solution unambiguously as a monomeric peptide based on molecular weight calculated from ultracentrifugation measurements.

These structural results are relevant to determining the optimal ratio of targeting peptide:Cy3-SA for hepatocyte targeting. A dose dependent decrease in targeted signal at MC893 to Cy3-SA ratios higher than 18:1 was observed, presumably due to competition for receptor binding by excess peptides (data not shown). Hepatocyte targeting of biotinylated p17 peptide:Cy3-SA complexes occurred most efficiently at the relatively high peptide to Cy3-SA molar ratio of 12:1 to 18:1 (molar ratio of 12:1 was used in results shown in Figure 3 and all results presented in Table 1). At ratios of lower than 9:1, the majority of Cy3-SA signals appeared to be on or near the basolateral membranes of hepatocytes and sinusoidal cell membranes, suggesting insufficient targeting activities (microscopy images not shown). SA molecules are tetrameric proteins, and therefore each has four biotin binding sites. The observation that efficient targeting required peptide to Cy3-SA ratios of 12:1 to 18:1 indicated that on average there were at least 3−4 peptides available per each biotin binding site. This assessment initially suggested that a certain trimeric peptide structural conformation is required for receptor interaction. However, since the biophysical characterization experiments indicated that p17 peptide exists as monomers with no α-helix- forming propensity, it is likely that receptor interaction is not dependent on the native p17 rod domain's α-helical trimeric coiled-coiled structure.

An analogous study evaluating the binding of biotinylated DNA fragment (152 bp) to SA provided an alternative explanation for the dependence on high biotin to SA ratios for p17 peptide-targeting activities.[26] In this study, using atomic force microscopy, it was observed that, at a biotinylated DNA fragment to SA molar ratio of 1:1, 75% of all SA evaluated had at least one biotin binding site occupied, with 58% of the SA molecules occupied by a single biotinylated molecule. At molar ratios of 10:1, 80% of all SA had at least one binding site occupied, with the majority of SA having either one (∼35%) or two (∼35%) biotin sites occupied.[26] Therefore, a relatively high biotin to SA ratio was needed to increase the percentage of SA with multiple

(26) Neish, C. S.; Martin, I. L.; Henderson, R. M.; Edwardson, J. M. *Br. J. Pharmacol.* **2002**, *135*, 1943−50.

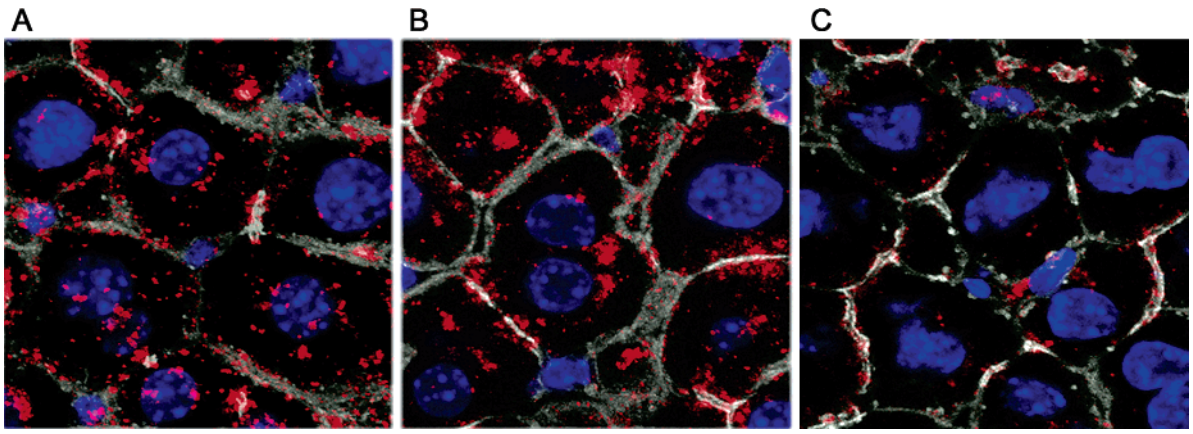

Figure 4. Hepatocyte targeting of biotinylated-Cy3-dextran (red, 70 kDa) by SA-p17 peptide conjugate. Liver samples were removed 10 min (A and C) and 20 min (B) after injection.

binding sites occupied. The authors also suggested that occupation of the first biotin binding site in a SA molecule may hinder subsequent occupation of the remaining binding sites and high concentration of ligand was needed to overcome the binding interference.[26]

Correspondingly, for our study, a relatively high molar ratio of p17 peptide to SA may be needed for biotinylated peptide to bind efficiently to SA and to increase the population of SA with multiple biotin sites occupied. SA with multiple biotin binding sites occupied would have a higher local peptide density and potentially higher targeting activities. This may emulate the native T7 phage tail complex where the conical tail tube was surrounded by six tail fibers, each tail fibers consisting of three p17 polypeptides,[21] and suggests that efficient targeting activities may require multivalent interaction of T7 peptide to its cell surface receptors.

Delivery of Biotinylated Cargo by SA-p17 Peptide Conjugates. A variety of cross-linking reagents and overall coupling strategies are available to link the targeting peptide to cargo. Since complete replacement of lysines with arginines disrupted targeting, it was not possible to employ cross-linking reagents that react with primary amines. Fortunately, the lack of cysteine residues within the targeting sequences allowed us to replace the N-terminus biotin of hepatocyte-targeting peptide MC893 with an N-terminal cysteine that would be available for sulfhydryl-reactive conjugation chemistry (MC892, Table 1).The overall coupling strategy is to chemically link this cysteine-containing MC892 peptide with SA, which can then be complexed with biotin-containing cargo (Figure 2B). The MC892 peptide was attached to SA that was modified with the heterobifunctional cross-linking reagent SPDP, which modifies amines to introduce a reactive pyridyl disulfide group (Pierce Biotechnology, Inc.). On the basis of release of pyridine-2-thione under reducing conditions, it was estimated that there were 8 PDP groups per SA tetramer, enabling a maximum of 8 MC892 peptides to be linked to a SA tetramer.

To test the hepatocyte-targeting activity of MC892-SA conjugate, biotinylated Cy3-labeled aminodextran (Cy3-dextran, 70 kDa) was mixed with MC892-SA conjugate at a biotin to SA molar ratio of 1:1. At 10 min after injection, a strong Cy3-dextran signal was seen inside hepatocytes with weaker signal near the basolateral membrane of hepatocytes (Figure 4A).

In contrast to using Cy3-SA as a reporter molecule, we were able to evaluate the targeting and hepatocyte uptake kinetics of Cy3-dextran since dextran is not readily degraded by lysosomal enzymes. At 20 min postinjection, Cy3-dextran signal was substantially decreased near basolateral membranes but increased as bright clusters near cell nuclei (Figure 4B). For control purposes, the hepatocyte targeting of complexes of unmodified SA and biotinylated Cy3-labeled aminodextran (biotin to SA molar ratio of 1:1, same ratio as the experimental samples) was evaluated (Figure 4C). Only a minor amount of unmodified SA/Cy3-dextran complexes was taken up by hepatocytes, indicating that the MC892 peptide was responsible for the robust uptake observed in the experimental samples.

Delivery by Direct p17 Peptide Conjugation. While the use of SA and biotin as a modular conjugation approach is well accepted in many applications, for some instances direct conjugation of p17 peptide to cargo may be preferred. The ability of the SA-MC892 conjugate to deliver biotinylated cargo to hepatocytes indicated that the unique cysteine residue in MC892 could be utilized for direct conjugation to cargo. When MC892 was directly linked to a fluorescent reporter molecule (thiol reactive Cy3 dye) to evaluate this conjugation approach, no Cy3-labeled peptide was detected in hepatocytes. This is likely due to the rapid removal of Cy3-labeled p17 peptide through renal clearance due to the small size of monomeric p17 peptide (3.7 kDa) and the likely rapid degradation of the peptide in endosomes. However, p17 peptide can be conjugated to various larger sized cargo and polymer supports to decrease renal clearance and can be used as a potential carrier system for targeted delivery of small molecules. A schematic representation of this conjugation approach is illustrated in Figure 2C. To demonstrate the hepatocyte-targeting utility of this conjugation approach, aminodextran was modified with SPDP to introduce reactive pyridyl disulfide group for peptide conjugation. It was

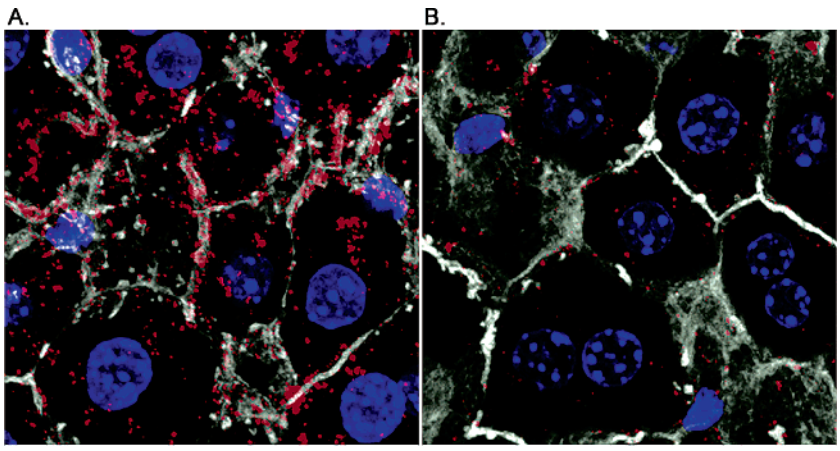

Figure 5. Hepatocyte targeting of dextran (red, 70 kDa) by covalent MC892 conjugation. Cy3-labeled, SPDP modified dextran (500 μg) was injected mixed with MC892 (A) or alone (B) into mice via the tail vein in 250 μL of Ringers solution. Liver samples were removed 10 min after injection.

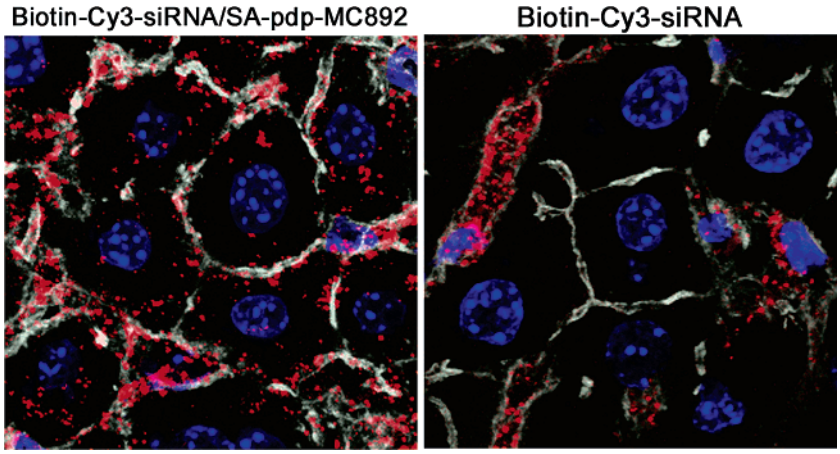

Figure 6. Hepatocyte targeting of biotinylated Cy3-siRNA by MC892-SA conjugate. Cy3-siRNA (red, 30 μg) was injected alone (panel on right) or mixed with MC892-SA (panel on left) in 250 μL of injection buffer via the tail vein into mice. Liver samples were removed 20 min after injection.

determined that on average 18 PDP groups per dextran molecule were attached. Dextran-PDP was mixed with a submaximal concentration of thio-modified Cy3 dye and MC892 (molar ratio of Cy3 dye to MC892 was 1:3, 75 mol % of PDP groups). Instead of the amino reactive Cy3 dye that was used to label dextran as described for the indirect delivery approach, disulfide reactive thio-Cy3 dye was used to simulate the effective attachment of disulfide reactive cargo. To ensure maximum conjugation of peptide and fluorophore, PDP groups were in molar excess. On the basis of the input MC892 ratios, each dextran molecule may have had up to10 MC892 peptides. In other studies, the presence of excess PDP groups was shown to have no effect on hepatocyte targeting.

Cy3-labeled MC892-dextran conjugate was injected into mice via the tail vein. At 10 min after injection, MC893 mediated a rapid accumulation of Cy3-dextran signal in mouse liver with the majority of the signal found within hepatocytes (Figure 5A). Similar to the indirect conjugation delivery approach, a small amount of nonspecific uptake was found in animals injected with Cy3-labeled dextran-PDP without MC892 addition (Figure 5B).

Delivery of siRNA to Hepatocytes. The MC892-SA conjugate was also tested for its ability to deliver biotinylated-siRNA to hepatocytes in mice in vivo. Biotinylated Cy3-labeled anti-luciferase siRNA was mixed with MC892-SA at a 1:1 molar ratio and injected into mice via the tail vein. At 20 min after injection, significant amounts of punctate Cy3-labeled siRNA signal were detected in mouse hepatocytes injected with hepatocyte-targeting MC892-SA conjugate whereas no signal was detected in control animals that received injections of solely Cy3-siRNA (Figure 6).[27] (Targeting of biotinylated siRNA by p17 peptide-SA conjugate (MC892) by normal tail vein injection was described in ref 27; however, it was erroneously quoted as delivered by hydrodynamic tail vein injection.) To determine if targeted siRNA mediated RNAi function in mice, the suppression of the liver specific peroxisome proliferator-activated receptor alpha (PPAR-alpha) gene expression was evaluated. At 24

(27) Henry, C. M. In *Chem. Eng. News* **2003**, *81* (51), 32−6.

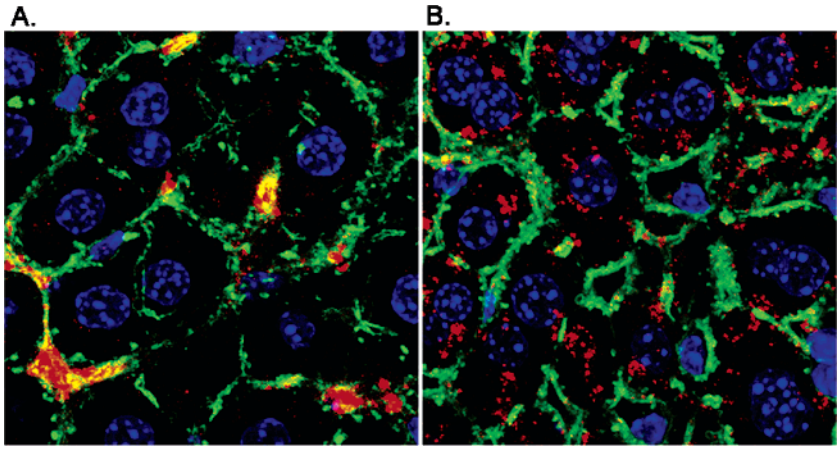

Figure 7. Hepatocyte delivery of fluorescent dye loaded liposomes (red). Liposomes (1.5 mg in 200 μL in 10 mM HEPES, 150 mM NaCl, pH 7.4) mixed with MC910-SA (nontargeting mutant p17 peptide conjugate) (A) and the hepatocyte-targeting MC892-SA conjugate (B) were injected via the tail vein into mice. Liver samples were harvested 30 min after injection. F-actin appears green, and cell nuclei are blue. Images represent 4 μm thick area of 75 μm^2.

h after injection, total RNA was extracted from liver and mRNA levels by real-time quantitative PCR assays were determined. The results of these experiments showed that MC892-SA targeted biotinylated anti-PPAR-alpha siRNA failed to invoke RNA interference activity in mouse livers. To determine if biotinylation of siRNA affects gene knockdown activities, the RNA interference function of biotinylated-siRNA (anti-luciferase) and SA conjugated biotinylated siRNA was tested using the siRNA transfection reagent, *Trans*IT TKO, in a mouse liver hepatoma cell line (hepalclc-7) that stably expresses the luciferase reporter gene (Hepa-luc). The transfection experiments showed that the gene knockdown activities of biotinylated siRNA or SA-conjugated biotinylated siRNA were not significantly different from siRNA without biotin modification. Since p17 peptide targeting is mediated by endocytosis, it is possible that targeted Cy3-siRNA may be trapped in endosomal compartments and unable to gain access to the cytoplasmic RNAi cellular machineries. Therefore, incorporation of an endosomal release strategy using this targeted delivery approach is likely to be required to achieve functional targeted siRNA delivery. This work is currently in progress.

Delivery of Particulate Cargoes: Liposomes. In addition to oligonucleotides and polymers, the ability of T7 peptide-SA conjugate to target biotinylated liposomes to hepatocytes was evaluated. Negatively charged, unilamellar liposomes were prepared containing DSPE-PEG2000-biotin, DSPE-PEG2000-methoxy, cholesterol, and DOPC (1:4:30:65, mol %). A small amount of Oregon Green-DHPE (0.5 mol %) was added for determining liposome concentrations. The liposomes were loaded with Cy3-hydrazine for in vivo targeting evaluation. Unincorporated Cy3-hydrazine was removed by size exclusion chromatography. Since the Cy3 fluorescence interfered with operation of the particle sizer, liposomes without Cy3-hydrazine were similarly prepared and found to have a diameter of 60 $\pm$ 13 nm. The ζ-potential of these liposomes was determined to be -25 ± 3 mV. After purification, Cy3-hydrazine loaded liposomes were injected into mice via the tail vein, and hepatocyte-targeting activities were determined by confocal imaging of Cy3-hydrazine fluorescence in liver cryosections. At 30 min after injection, Cy3-hydrazine containing biotinylated-liposomes were efficiently targeted to mouse hepatocytes by MC892-SA conjugate (Figure 7B). Compared to Cy3-SA, dextran, or siRNA, the larger sized liposome had a slower uptake rate; therefore, liver samples were collected at 30 min to allow maximal uptake to occur while signal degradation was at the minimal. High levels of the signal were found within hepatocytes with only a relatively small amount of signal associated with sinusoidal cells. In contrast, minimal Cy3-hydrazine signals were detected in mouse hepatocytes injected with liposomes containing the nontargeting peptide MC910-SA conjugate (Figure 7A). Most of the signal was found clustered in sinusoidal cells.

Delivery of Particulate Cargoes: Nucleic Acid Complexes. Liposome targeting demonstrated the ability to target nanoparticles; the ability of T7 peptide to target DNA-polycation polyplexes to hepatocytes was also evaluated. The DNA complexes were prepared using the synthetic polyamine pBAVE,[22] at a polymer to DNA weight ratio of 4:1, that was covalently cross-linked with glutaraldehyde to increase the stability of the complexes in physiologic salt solutions.[28,29] This process is also known as caging. The polymer pBAVE was also modified with biotinylated-PEG5000 (pBAVE-biotin) for MC893-SA conjugate attachment. After the complexes were cross-linked, they were PEGylated to reduce their positive charge and decrease their nonspecific interactions with serum proteins and cells. Their average size was $\sim$60 nm in diameter with a ζ-potential less than 5 mV. The addition of the MC893-SA conjugate to complexes substantially increased their hepatocyte targeting (Figure 8A,B). For

(28) Adami, R. C.; Rice, K. G. *J. Pharm. Sci.* **1999**, *88*, 739−46.
(29) Trubetskoy, V. S.; Loomis, A.; Slattum, P. M.; Hagstrom, J. E.; Budker, V. G.; Wolff, J. A. *Bioconjugate Chem.* **1999**, *10*, 624−8.

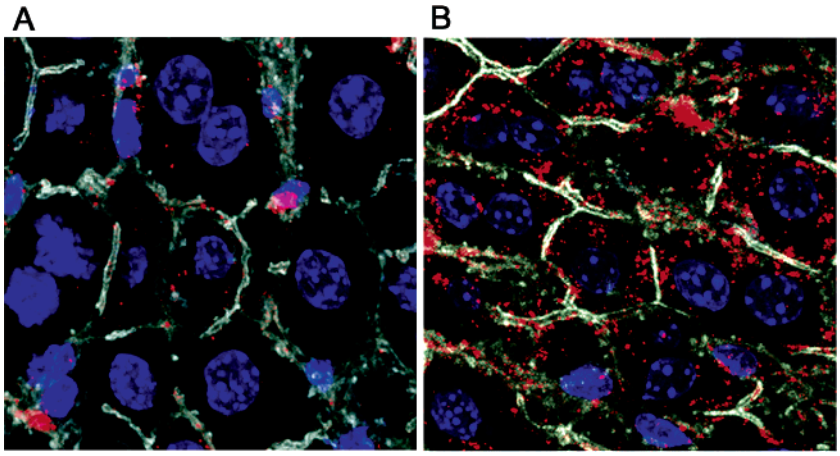

Figure 8. Targeted delivery of biotin containing Cy3-labeled DNA complexes (red) to mouse hepatocytes. (A) DNA complexes alone. (B) Complexes with targeting conjugate added (5 μg of MC892-SA). DNA complexes were injected into mice via the tail vein, and liver samples were removed 1 h after injection.

nucleic acid complex uptake, optimal uptake occurred at 1 h after injection. Although the DNA complexes and liposomes were similar in size, the DNA complexes appeared to be taken up more slowly by the hepatocytes. This suggests that factors other than cargo size, e.g., serum stability and net surface charges, may also affect the rate of uptake. Nevertheless, these results validated the functional utility of p17 peptides as a hepatocyte-targeting signal for delivering DNA complexes. Since the caging process prevents release of the DNA, efforts are in process to develop labile cross-linkers that would enable targeting and gene expression.

Summary

The hepatocyte-targeting determinant of the T7 p17 protein was mapped to a peptide of 33 residues derived from the rod domain. The peptide was able to target small molecules, proteins, siRNA, DNA polyplexes, and liposomes to hepatocytes. While biophysical studies indicated that the peptide did not form a triple α-helical, coiled-coil structure like the native p17 rod domain, multivalent receptor interaction appeared to be required for activation of uptake mechanism. This is the first description of a hepatocyte-targeting peptide, and thus the peptide can be chemically synthesized, which reduces the time and cost of ligand production and facilitates the incorporation of functional groups for cargo conjugation chemistry. The ability to use a variety of coupling strategies and chemistries better enables the cargo to be delivered without having its biologic activity inactivated by the conjugation process. Further studies are in progress to use this versatile system to provide functional activity of delivered nucleic acids by enabling their endosomal escape. Finally, this peptide domain could also be incorporated into viral vectors, either genetically or chemically.

Note Added after ASAP Publication. There was an error in Figure 2B in the version published ASAP on March 28, 2006; the corrected version was published on July 12, 2006.

Acknowledgment. This work was supported in part by the National Institutes of Health (DK064469 and DK0650900).

MP050108R